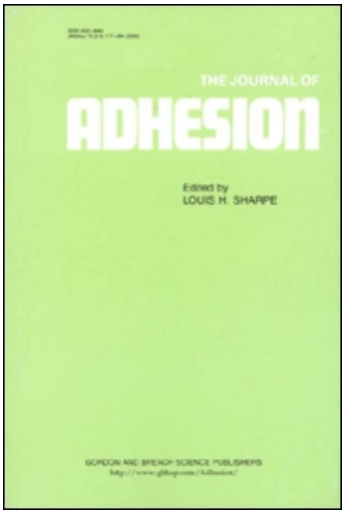

The Journal of Adhesion
Publication details, including instructions for authors and subscription information:
http://www.informaworld.com/smpp/title~content=t713453635

Adhesion at Polymer-Solid Interfaces: Influence of Sticker Groups on Structure, Chain Connectivity and Strength

Liezhong Gong[a]; Richard P. Wool[ab]
[a] Department of Chemical Engineering, University of Delaware, Newark, DE, USA [b] Center for Composite Materials, University of Delaware, Newark, DE, USA

To cite this Article Gong, Liezhong and Wool, Richard P.(1999) 'Adhesion at Polymer-Solid Interfaces: Influence of Sticker Groups on Structure, Chain Connectivity and Strength', The Journal of Adhesion, 71: 2, 189 — 209
To link to this Article: DOI: 10.1080/00218469908014848
URL: http://dx.doi.org/10.1080/00218469908014848

J. Adhesion, 1999, Vol. 71, pp. 189–209
Reprints available directly from the publisher
Photocopying permitted by license only

Adhesion at Polymer-Solid Interfaces: Influence of Sticker Groups on Structure, Chain Connectivity and Strength*

LIEZHONG GONG [a] and RICHARD P. WOOL [a,b,†]

[a] *Department of Chemical Engineering, University of Delaware, Newark, DE 19716, USA;*
[b] *Center for Composite Materials, University of Delaware, Newark, DE 19716, USA*

(Received 11 February 1999; In final form 7 May 1999)

The influence of sticker groups (COOH) on the adhesion energy (G_{IC}) of a model carboxylated polybutadiene-amine terminated silane modified aluminum (cPBD-AlS) interface was examined using a *T*-peel test. An optimal COOH concentration of around 0.5 mol% was observed. At this concentration the interface possessed a maximum peel energy of 600 J/m^2, which is approximately equal to the cohesive peel energy of PBD. The adhesion strength of the interface increased as the interaction parameter (χ_{P-S}) between COOH and the solid substrate increased. Additionally, G_{IC} was strongly dependent on the annealing time, resulting from slow surface reorganization processes. The interface structure was explored using the self-consistent field lattice model (SCFLM) developed by Theodorou. An interphase region adjacent to the solid substrate was found as a consequence of a gradient in chain connectivity and a strong sticker group segregation near the solid surface. The modeling study provided information about how the interphase structure changed with ϕ and χ_{P-S}, explaining the experimental results well.

Keywords: Interphase; interface; adhesion; self-consistent field; polybutadiene

*Abstract presented to Materials Research Society, Boston, MA, USA, December 1997.

†Corresponding author. Tel.: 302-831-3312, Fax: 302-831-1048, e-mail: Wool@ccm.udel.edu

1. INTRODUCTION

The synthesis and performance of polymer-solid interfaces are crucial for many modern technologies [1 – 6]. Fiber-reinforced composites [3], biomedical implants [4], targeted gene delivery [5], and packaging for microelectronics components [6] are a few examples that are dependent on the integrity of such interfaces. Although different properties are desirable for different applications, obtaining strong adhesion is an issue of fundamental importance because it plays a critical role in determining the properties, function, and reliability of the interface systems. The adhesion strength of a polymer-solid interface is controlled by two correlated principal factors: (1) the extent of polymer chains adsorbed onto the solid substrate and (2) the connectivity between adsorbed chains and non-adsorbed chains [7]. The interaction between the adsorbed polymer chains and the solid substrate can be improved by incorporating sticker groups onto the chains [7]. These sticker groups interact with the solid substrate strongly through hydrogen, ionic, or chemical bonding, resulting in better adhesive strength. However, the addition of sticker groups also perturbs the chain connectivity between the adsorbed chains and the non-adsorbed chains and modifies chain dynamics at the interface.

While several distributions of sticker groups on the polymer chains may exist, here we only consider one important case: sticker groups randomly located along the whole length of the polymer chain, as illustrated in Figure 1. From a fundamental point of view, the fracture energy, G_{IC}, of such polymer-solid interfaces is controlled by the polymer areal density (Σ), chain length (N), sticker group concentration (ϕ), the interaction strength between sticker groups and the solid

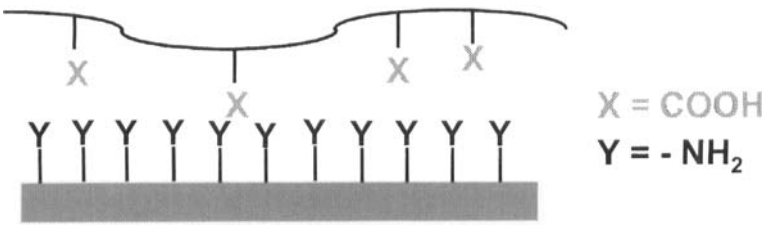

FIGURE 1 Illustration of a polymer-solid interface with sticker groups (X) distributed randomly along a polymer chain.

substrate (χ_{P-S}), as well as bonding time (t). The fracture energy of such polymer-solid interfaces at a constant test condition can be related to these molecular details by [7]:

$$G_{IC} = f(H) = F\{N, \Sigma, \phi, \chi_{P-S}, t\} \quad (1)$$

where H represents the interface structure.

In recent years, considerable attention has been devoted to understanding the influence of N and Σ by examining (1) immiscible polymer–polymer interfaces containing di-block or random copolymer additives [8–13] and (2) polymer-solid interfaces with tethered polymer chains [14–17]. It is quite well understood how the values of N and Σ affect the micro-mechanical deformation processes and how they impact the interface strength. For example, Creton *et al.* [12] have examined the interfaces between poly(2-vinylpyridine) (PVP) and polystyrene (PS) reinforced with block copolymer poly(styrene-b-2-vinylpyridine). When the PVP block length (N_{PVP}) of the copolymer is short and Σ is low, the interfaces fail by pull-out of the PVP block and G_{IC} scales with Σ and $N_{PVP}{}^2$, respectively. When both blocks (N_{PS} and N_{PVP}) are long and Σ is low, the interfaces fail through chain scission and G_{IC} scales with Σ. If N_{PS} and N_{PVP} are long and Σ is high, the interfaces fracture by first forming stable crazes, resulting in much higher values of G_{IC} in proportion to $\Sigma_{eff}{}^2$ (an areal density of chains with at least one "effective" entanglement). Deruelle *et al.* [14, 15] have reported the adhesion energy between polydimethylsiloxane (PDMS) and flat silica modified by irreversible adsorption and end grafting PDMS chains using a JKR experiment. It is found that G_{IC} passes through a maximum with increasing Σ, as a result of various capabilities of the grafted chains to penetrate into the PDMS network. Lin *et al.* [16, 17] have explored the interfaces between polysulfone and glass fiber modified by end-tethered polysulfone chains using a single filament pull-out experiment. The influence of the N, Σ, as well as the length polydispersity of the end tethered chains has been investigated. They conclude that the improvements in interfacial toughness were a result of the increased mixing between the tethered chains and the matrix chains.

However, the influence of the other two important parameters, ϕ and χ_{P-S} of Eq. (1), on interface structure and strength is not

fundamentally understood yet. In a previous paper [7], we have examined the influence of sticker group concentrations by investigating model carboxylated polybutadiene-aluminum (cPBD-Al) interfaces. In this interface the carboxylic acid (COOH) groups are distributed randomly through the entire length of polymer chains and act as sticker groups forming hydrogen bonding with the Al (Al_2O_3) substrate. Counter-intuitively, our preliminary results indicate that the peel energy of cPBD-Al interfaces is not a monotonic function of the COOH content (ϕ) as shown by Figure 2. An optimal COOH concentration (≈ 3 mol%) exists for cPBD-Al interfaces giving rise to a maximum G_{IC}. The occurrence of such an optimal COOH concentration is related to the formation of a weaker interphase region resulting from variation in polymer chain connectivity near the solid substrate. Essentially cPBD-Al interfaces with $\phi > \phi_c$ possess cPBD chains that are adsorbed too densely on the solid substrate and, thus, prohibit efficient entanglement (connectivity) between the adsorbed chains in contact with the solid substrate and the non-adsorbed chains. While, at $\phi < \phi_c$,

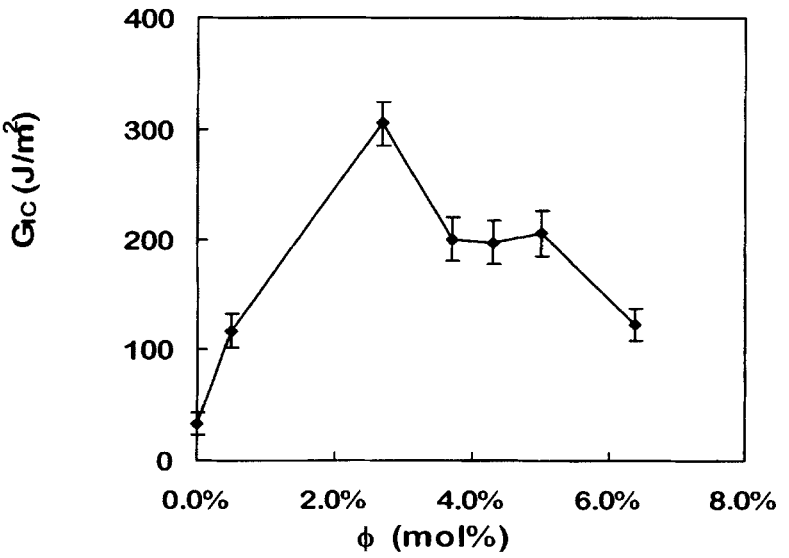

FIGURE 2 Influence of sticker groups concentrations (ϕ) on the peel energy (G_{IC}) for cPBD-Al interfaces annealed for 1000 min at room temperature.

the interface strength is limited by the adhesive strength. Therefore, the more the sticker groups, the stronger the interfaces.

An interphase is a three-dimensional transition zone between the solid substrate and the polymer bulk [18–27]. The thickness of an interphase region can vary from just several atomic layers near the solid surface to a few microns [18]. It has been well established that the properties of polymers in the interphase are generally different from those in the bulk [19–22, 26]. The presence of an interphase region could be the result of segregation of low molecular weight polymer chains, different coefficients of thermal expansion between the polymer and the solid, migration of the low molecular weight processing additives, preferential adsorption of one specific component, or surface induced crystallization [19, 21, 24–27]. However, reports of an interphase caused by variation of chain connectivity are quite few.

In this paper, we present new data supporting the existence of an interphase region at polymer-solid interfaces resulting from the perturbed chain connectivity. We first explore the influence of χ_{P-S} and ϕ (the last two terms of Eq. (1)) on the fracture energy by examining cPBD-amine terminated silane modified aluminum (cPBD-AlS) interfaces. A self-consistent field lattice model (SCFLM) developed by Theodorou is then employed to elucidate the origin of the interphase. Finally, a schematic model is proposed to represent the interphase microstructure based on the experimental and simulation results.

2. EXPERIMENTAL

2.1. Model Polymers

Carboxylated polybutadienes with varying concentrations of COOH (0–6 mol%) were used as model polymers. These polymers were synthesized through high pressure hydrocarboxylation of polybutadiene (Diene 35 AC 10, supplied by Firestone Company with M_n = 98,000, M_w = 182,000) [28]. No significant chain scission or crosslinking was detected during the reaction and the distribution of COOH was random along the polymer chains. As listed in Table I, the glass transition temperature is only slightly above that of the corresponding PBD.

TABLE I The glass transition temperatures of carboxylated polybutadienes (cPBD) with different COOH concentrations

—COOH (mol%)	0.0	0.5	0.7	0.9	2.7	3.6	4.5	5.1
T_g (°C)	−96	−95.5	−95	−94	−89.5	−88.5	−86.5	*

* no significant glass transition observed.

2.2. Model Substrates

Aluminum foil (25 μ thick and average roughness ≈ 0.5 μ manufactured by Shop-Aid Inc., MA) modified with amine-terminated silane was employed as the model substrate. The pretreated Al foil was first baked at 300°C under atmospheric air overnight to remove simultaneously any possible organic contaminants and form a stable layer of oxide. As shown in Figure 3, after this treatment, the C-1s peak on the X-ray photoelectron spectroscopy (XPS) spectrum was significantly reduced, which means most of the organic contaminants had been removed. The treated foil was then uniformly coated with a layer of aminoethylaminopropyl trimethoxysilane (Dow Corning z-6020) by dipping into an aqueous solution (0.5 wt%) of the silane for 5 min. The pH of the silane solution was held at approximately 5.5 by the addition of drops of acetic acid. Subsequently, the silane-coated Al foil was dried in the air and followed by cross-linking at 110°C under N_2 and vacuum for half an hour each. As illustrated in Figure 3, signals from C, Si, O and Al can be observed clearly on the XPS spectrum of the amine terminated silane coated Al foil.

2.3. Model Interfaces

The model cPBD-AlS interfaces were prepared by solution-casting a uniform, thin cPBD layer onto the amine-terminated silane coated Al foil. The type of interaction between sticker groups (—COOH) and amine on the solid substrate is believed to be ionic at room temperature. This is because —COOH and —NH_2 can be easily ionized to —COO^- and —NH_3^+ at ambient temperature when they approach each other. The interaction of cPBD-AlS interfaces has a strength of $\chi_{P-S} \approx 20$ [29], which is much higher than the hydrogen bonding strength for cPBD-Al interfaces ($\chi_{P-S} \approx 6$) as reported earlier [7].

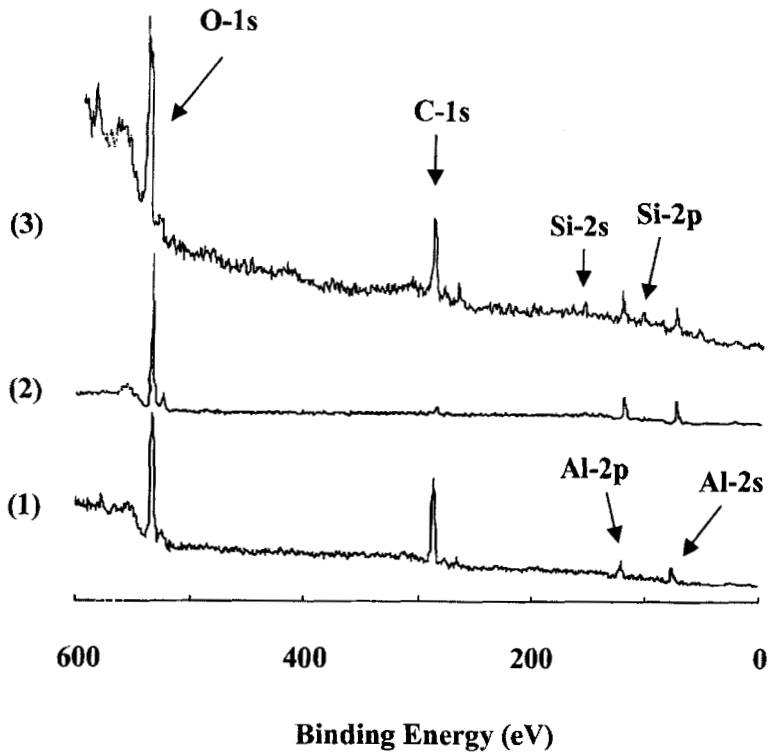

FIGURE 3 XPS survey scans of aluminum substrates: (1) Al before baking, (2) Al after baking for 20 hr at 300°C under atmospheric air, (3) silane-modified Al (AlS).

2.4. Peel Energy of the Model Interfaces

The peel energy, G_{IC}, of the cPBD-AlS interfaces was evaluated by a *T*-peel test as illustrated in Figure 4. A layer of cPBD was uniformly cast onto the amine-terminated silane coated Al foil from a 1 wt% toluene solution. The thickness of the cPBD layer was kept around 15 μm by controlling the solution volume cast and the surface area covered. The toluene solvent was allowed to evaporate under atmospheric pressure and further dried under vacuum for 15 min. After this process, the second amine-terminated, silane-coated Al foil was put onto the top of the cPBD layer to form an AlS-cPBD-AlS sandwich structure. These AlS-cPBD-AlS interfaces were pressed together for 5 min to ensure good contact and then annealed under 4 kPa

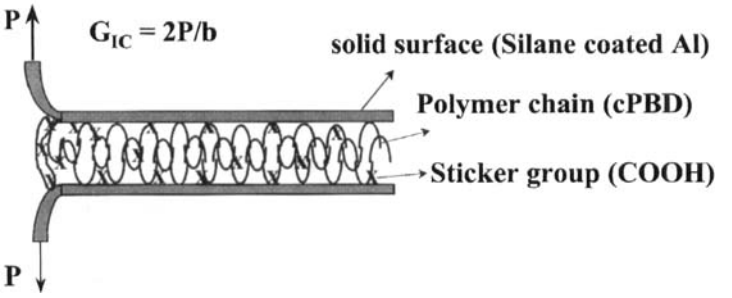

FIGURE 4 Schematic representation of the *T*-peel test employed to evaluate the peel energy of cPBD-AlS interfaces.

of pressure at room temperature for different lengths of times. The samples for the peel test were cut from this into strips 60 mm in length and 10 mm in width. The peel tests were carried out on a Mini-44 Instron tensile machine at a cross-head speed of 30 mm/min. The peel energy, G_{IC}, was obtained from the average of 3 tests per material, and was calculated by:

$$G_{IC} = \frac{2P}{b} \tag{2}$$

where P is the peel load and b is the width of the test sample.

2.5. Modeling Study of the Interface Structure

A self-consistent field lattice model (SCFLM) simulation developed by Theodorou [30, 31] was employed to explore the interface structure. The SCFLM used is essentially an extension of Flory-Huggins' theory on thermodynamics of mixing applied to anisotropic polymer melts at sharp interfaces, *e.g.*, polymer-solid interfaces. It has been shown that this model is capable of generating very important information about interface structure, such as the concentration distribution of sticker groups and the shape of polymer chains at a polymer-solid interface [31]. The computation was done using the software from Biosym/ Molecular Simulations [32]. Further details on the modeling can be found elsewhere [7, 30, 31].

2.6. XPS and SEM Analysis

Solid substrates and the fresh fractured surfaces were characterized by XPS and SEM. XPS analysis was carried out on a Leybold-Heraeus spectrometer equipped with a hemispherical electron energy analyzer and a Mg Kα source operating at 10 kV and 10 mA. The equipment was calibrated with Au 4*f* and Cu 3*p* lines. The pressure in the sample chamber was maintained at around 10^{-9} Torr. SEM micrographs of the fractured surfaces were obtained with a JEOL 840 microscope operated at 3 kV. The fractured polymer surfaces were sputtered with gold under 25 mA for 1 min.

3. RESULTS AND DISCUSSION

3.1. Influence of Sticker Group Concentration

The influence of sticker group concentrations (ϕ) on the peel fracture energy (G_{IC}) is shown in Figure 5. A long annealing time, around 1000 minutes, was kept for all interfaces to ensure equilibrium. It is apparent that G_{IC} initially increases with ϕ up to 0.5 mol%. But, after a critical value of $\phi_c \approx 0.5$ mol%, the peel energy decreases with further increase of ϕ, giving rise to an optimal concentration for maximum adhesion at the cPBD-AlS interface. At $\phi_c \approx 0.5$ mol%, significant deformation of cPBD was observed during the peel test and residual polymer was visible by SEM on both sides of the fractured interfaces as shown in Figure 6. For cPBD-AlS interfaces with ϕ other than ϕ_c, deformation of cPBDs was much less severe. However, after examining the fractured surfaces by XPS, polymer residual was still detected on both sides and the loci of failure were found mainly in the region near the second Al substrate.

It has been generally believed that an *S*-like curve for G_{IC} *vs.* ϕ should be obtained [33]. With increasing ϕ, the strength of the interface should increase gradually and eventually approach a plateau close to the cohesive strength of the bulk polymer. However, others have observed the phenomenon of maximum adhesion at critical concentrations, as reported here, when investigating the adhesion of copolymers to various solid substrates [34–36]. These results were attributed to factors such as crystallization of copolymers [34], excess corrosion

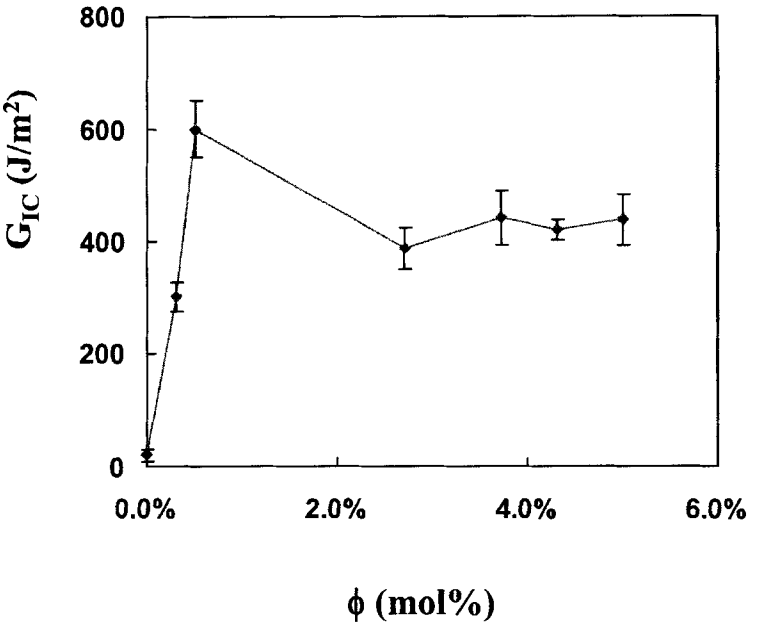

FIGURE 5 Influence of sticker group COOH concentrations (ϕ) on the peel energy (G_{IC}) of cPBD-AlS interfaces, indicating an optimal concentration (ϕ_c)$\approx$0.5 mol% (annealing time: 1000 min at ambient temperature).

of the solid substrates [35], and polymer chain scission [36] associated with further increase in the surface-sticky components. However, none of these explanations can justify the results obtained in the present study. As pointed out in the experimental section, the cPBDs used are amorphous with T_g's much lower than room temperature, indicating that no crystallization should exist. The hydrocarboxylation reaction does not change the molecular weight significantly [28] and corrosion of the solid substrate was not observed after the peel test. Therefore, the cause for the maximum adhesion phenomenon in the cPBD-AlS system is different from those presented in the past.

As pointed out in the previous section (Fig. 2), for cPBD-Al interfaces we also observed a critical concentration of sticker groups, ϕ_c, around 3 mol% leading to adhesion energy around 300 J/m^2. We interpreted this result as a consequence of the most efficient chain entanglement between the near-surface adsorbed polymer layer and the far-surface, non-adsorbed polymer layers in the interphase region.

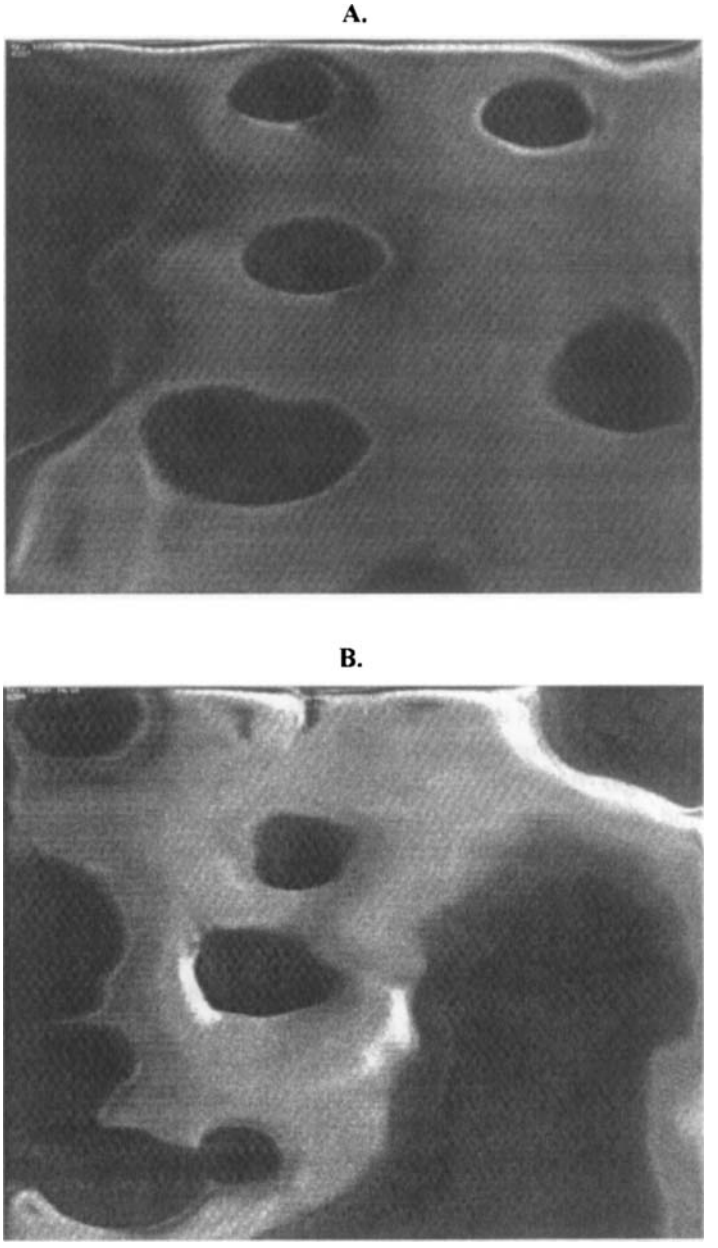

FIGURE 6 SEM micrographs of fractured surfaces (sides A and B) for cPBD-AlS with $\phi = 0.5$ mol% and annealing for 1000 min at room temperature (magnification 200).

Such an argument has also been proposed by several other researchers [36–39] and can be further supported by our modeling studies [7], which will be discussed in detail. Similar to cPBD-Al interfaces, we suspect that the dependence of G_{IC} on ϕ for cPBD-AlS interfaces is mainly caused by a variation of entanglement chain connectivity within the interphase region.

The influence of χ_{P-S} on the interface strength can be observed through detailed examination of the difference between Figures 2 and 5. First, ϕ_c shifts from a value of ≈ 3 mol% for cPBD-Al to a lower value (≈ 0.5 mol%) for cPBD-AlS. Secondly, at the same COOH concentrations, the value of G_{IC} of cPBD-AlS interfaces is higher than that of cPBD-Al interfaces. An additional observation is that the corresponding peel energy for cPBD-AlS at ϕ_c is around 600 J/m^2, which is close to the cohesive peel energy of PBD as obtained by others [40].

3.2. Bonding Dynamics

Bonding dynamics is a key issue since it controls how fast an interface can develop mechanical strength. This development in the cPBD-AlS interfaces can be seen in Figure 7, where the peel energy has been evaluated at various annealing times. We can see that the peel energy increases with annealing time up to 100 minutes, which is actually much longer than the characteristic relaxation time of PBD bulk (around 20 seconds at room temperature) [7]. We believe that this phenomenon is caused by a frustrated surface reorganization process, which is affected by ϕ and χ_{P-S} [41]. With further increase in annealing time up to about 2000 minutes, the peel energy does not change considerably.

Bonding dynamics at a polymer-solid interface is determined by several steps including wetting of the solid substrate by polymer melt, formation of bonds between the sticker groups and the solid surface, and reorganization of surface polymer chains to equilibrium [2, 7]. For cPBD-AlS interfaces, because the cPBD polymer is a rubber with low T_g, full wetting contact between the polymer and the solid substrate was achieved by pressing them together before annealing. During annealing, the COOH groups have to diffuse and adsorb to the solid substrate through strong interactions between the sticker groups and the —NH_2 groups. Once a COOH group from a PBD chain is

adsorbed to the solid substrate, the chain's mobility is severely restricted. An adsorbed chain is composed of loops and tails as illustrated by Figure 8. Without breaking the adsorption sites, loops will relax through restricted Rouse dynamics, while the tails can be

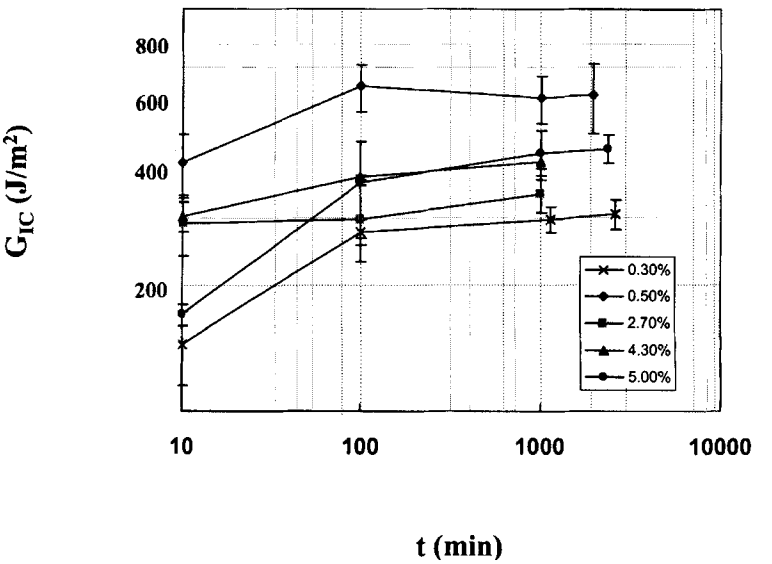

FIGURE 7 Dependence of the peel energy (G_{IC}) of cPBD-AlS interfaces on the annealing time (t) at ambient temperature. COOH concentration: × 0.3 mol%, ◆ 0.5 mol%, ■ 2.7 mol%, ▲ 4.3 mol%, ● 5.0 mol%.

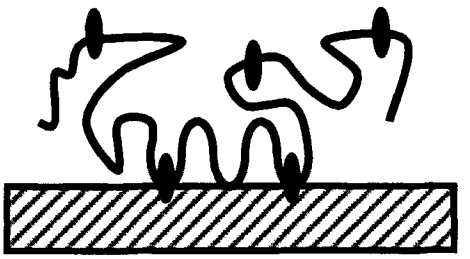

FIGURE 8 An adsorbed chain is composed of loops and tails. Without breaking the adsorption sites, dynamics of tails can be described, in part, by the dynamics model of end-tethered polymer chains.

considered as end-tethered chains with a very long relaxation time. Consequently, as a first approximation, the dynamics of an adsorbed chain can be described, in part, using the dynamics model of end-grafted chains.

O'Connor and McLeish have examined the dynamics of end-grafted chains approaching their equilibrium conformation after being brought into contact with the same bulk polymer [42]. In this case, three dynamical regimes were identified: (1) fast Rouse-like penetration, (2) retraction of the free ends, and (3) slow diffusive dynamics. The characteristic relaxation time (τ_R) for the third regimes was expressed as:

$$\tau_R \approx \tau_{N_t} \exp\left(\frac{\alpha^2 b^2 N}{6a^2}\right)\left[1 - \exp\langle -\pi(\gamma - \gamma_0)R_0\rangle\right]$$

$$\text{where } \gamma_0 = \sqrt{\left(\frac{1}{d^2} - \frac{2}{a^2} + \frac{6\varphi_{\text{eff}}\chi}{\pi b^2}\right)}$$

$$\text{and } \gamma = \sqrt{\left(\frac{1}{d^2} - \frac{(2 - \alpha^2/\pi^2)}{a^2} + \frac{6\varphi_{\text{eff}}\chi}{\pi b^2}\right)} \tag{3}$$

The parameters in the above equation are, a, the characteristic distance between network topological constraints (consisting of around 30 structure units for PBD), b, the monomer dimension (~ 5 Å for PBD), d, the width of an unentangled layer of the network material, R_0, the tunneling distance, N_t, the number of monomers penetrating into the bulk polymer, ϕ_{eff}, the effective grafted-chain surface density and, χ, the Flory parameter describing direct interaction with the solid surface, respectively.

It has been reported that the relaxation time (τ_R) calculated in this manner is several orders of magnitude longer than the characteristic relaxation time of polymer bulk [42], which is consistent with our experimental observation for cPBD-AlS interfaces.

Compared with cPBD-Al interfaces, we found that adhesion in cPBD-AlS interfaces develops faster for all ϕ, possibly resulting from the stronger interaction parameter, $\chi_{\text{P-S}}$. Additionally, the dependence of the interface reorganization rate on the sticker group concentrations shown by cPBD-Al interfaces, is not observed for cPBD-AlS interfaces [7].

3.3. Structure of Polymer-Solid Interfaces: An SCFLM Study

In order to understand further the experimental results, a simulation study was used to investigate the structure and chain connectivity of the polymer-solid interfaces. This was done using the SCFLM developed by Theodorou [30, 31]. The distribution of sticker groups (ϕ_{Ai}) at a model polymer-solid interface with $N = 100, \phi = 3\,\text{mol}\%$ and $\chi_{P-S} = 2.5$ is illustrated in Figure 9. The structure of the adsorbed chain was also determined and expressed in terms of average number of segments per chain at layer i, $N_{si}(z)$, as shown in Figure 10. N_{si} is a sensitive measure of the local chain structure and is related to the areal chain density, Σ, by

$$N_{si} \propto \frac{1}{\Sigma} \tag{4}$$

Therefore, a high value of N_{si} represents a flatter chain with lower areal chain density at the ith layer, while a lower value of N_{si} indicates that chains are more densely populated and are stretched perpendicularly to the solid substrate.

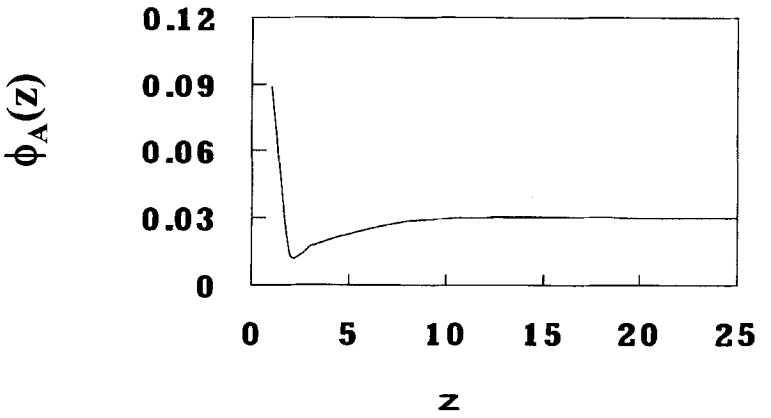

FIGURE 9 Sticker group distribution at a model polymer-solid interface computed from the SCFLM. z: the distance from the solid surface, $\phi_A(z)$: the local sticker group concentration at z layers away from the solid substrate. Interface parameters: polymer chain length $N = 100$, sticker group concentration in the bulk $\phi_{A\ Bulk} = 3\,\text{mol}\%$, interaction strength between sticker groups and the solid substrate $\chi_{A-S} = 2.5$, interface thickness $L = 50$.

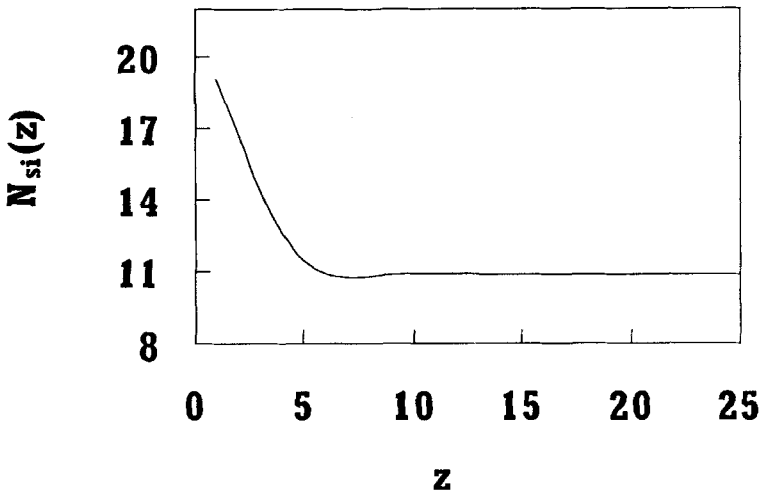

FIGURE 10 Chain shape distribution at a model polymer-solid interface computed from the SCFLM. z: the distance from the solid surface, N_{si}: chain shape parameter, the average number of segments per chain at layer i. Interface parameters are the same as those in Figure 9.

Additionally, the number of layers a chain can cross in the z direction (perpendicular to the solid substrate), R_z, is related to N_{si} and N by

$$R_z \propto \frac{N}{N_{si}} \tag{5}$$

In the polymer bulk, as a result of random walk, we have

$$N_{si} \propto N^{0.5} \tag{6}$$

From Figures 9 and 10, we can see that both the sticker group distribution and the chain shape at the region near the solid surface are significantly perturbed. The sticker groups segregate to the solid surface and the chains flatten at the near-solid substrate layers with larger N_{si}, forming a three-dimensional interphase region with different properties from the polymer bulk. The presence of such an interphase zone is a consequence of the interplay between the competition

for adsorption of the sticker groups to the solid surface and the impenetrable boundary condition imposed by the solid substrate. Based on the modeling result, a schematic representation of the polymer-solid interface is given in Figure 11, with loops representing polymer chains and shaded background representing the sticker group distribution. The region near the solid substrate is darkly shaded signifying a high sticker group concentration. Past this region is a sticker-group-deficient region denoted by less shaded background. The chains (loops) in the interphase are flatter and then extend to shorter distances in the z-direction than those in the bulk. Additionally, compared with the polymer bulk, loops within the interphase have shorter

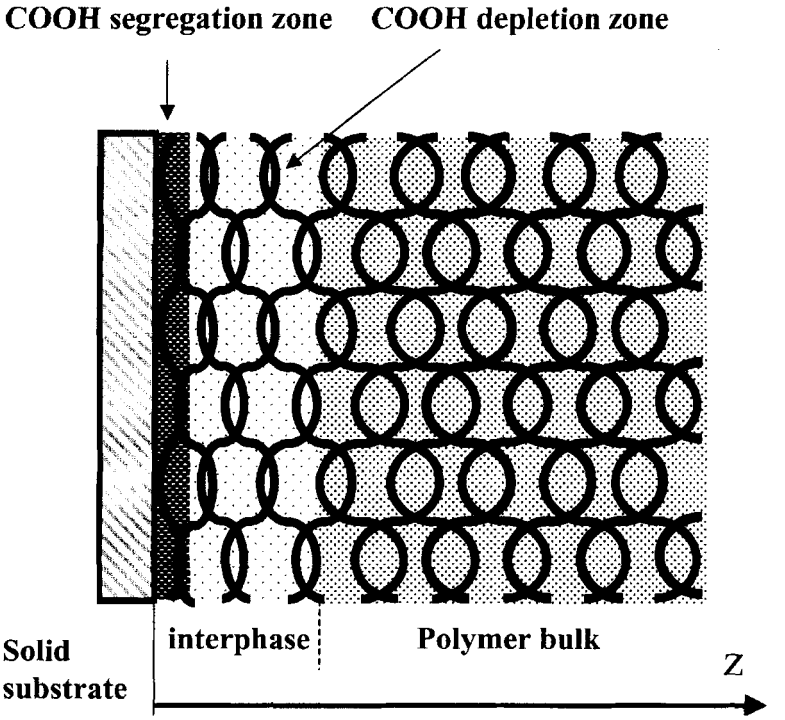

FIGURE 11 Schematic representation of a polymer-solid interface structure, shaded background: sticker groups, loops: polymer chains. An interphase region exists adjacent to the solid surface as a result of sticker group segregation and chain shape perturbation.

penetration lengths (overlaps) with the adjacent loops in the z-direction, leading to less efficient chain interpenetration, lower connectivity and, therefore, poorer strength in general.

Thus, during the peel test, a crack can propagate along the interfacial line, within the interphase region, or through the bulk polymer depending on the relative magnitude of the adhesive strength (σ_A), the interphase cohesive ($\hat{\sigma}^I$) and yield strength (σ_y^I), as well as the bulk polymer cohesive ($\hat{\sigma}^B$) and yield strength (σ_y^B). For example, when σ_A is the lowest, pure adhesive failure occurs as in PBD-AlS interfaces with $\phi = 0\%$. When $\hat{\sigma}^I \approx \hat{\sigma}^B$ but are much smaller than σ_A, cohesive failure is observed and the interface approaches the strength of the polymer bulk as in the case of cPBD-AlS interfaces with $\phi = 0.5\%$. However, for most cPBD-AlS interfaces, the interphase region is the weakest (low $\hat{\sigma}^I$) and cracks propagate through this weak region.

We have shown that the structure of such interfaces and the chain connectivity in the interphase region is a function of N, χ_{P-S} and ϕ [7]. Specifically, the relationship between N_{si} and ϕ at a constant χ_{P-S} is not monotonic. With increasing ϕ at a constant χ, we have shown (Fig. 11 of Ref. [7]) that there exists a critical concentration, ϕ_c. At this concentration the adsorbed polymer chains and segments in the interphase region are most efficiently connected with the non-adsorbed chains, creating a maximum bonding energy for the interface. The experimental results of G_{IC} *vs.* ϕ for cPBD-AlS interfaces are consistent with this modeling prediction and indicate that $\phi_c \approx 0.5$ mol%.

The influence of χ_{P-S} on chain connectivity in the interphase region is shown in Figure 12. At a constant ϕ, the values of N_{si} in the interphase region approach that in the bulk as χ_{P-S} increases, indicating more efficient connectivity and then a stronger bonding energy for the interface with a higher χ_{P-S}. What happens here is that a strong interaction will lead to a large segregation of the sticker groups, which, in turn, will cause more loops between the interfacial layer and the rest of the polymer chains and, therefore, stronger adhesion strength. This result explains why, at the same sticker group concentration, cPBD-AlS interfaces with a high χ_{P-S} have a better peel energy than cPBD-Al interfaces with a lower χ_{P-S}.

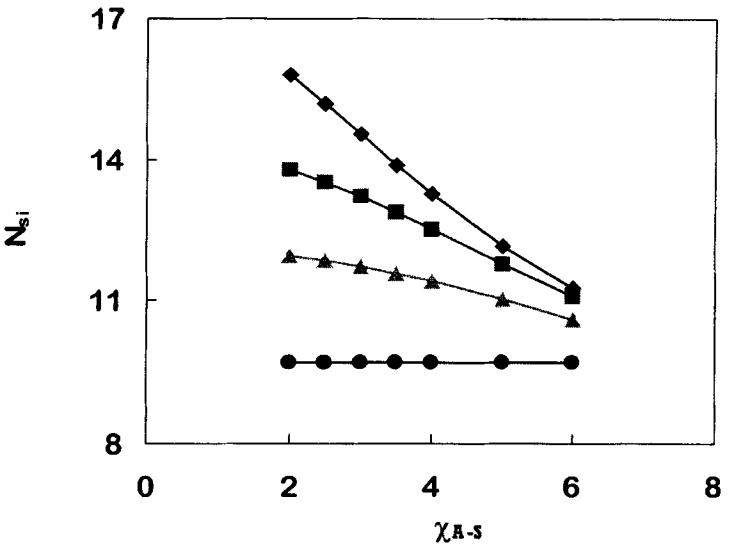

FIGURE 12 Influence of χ_{A-S} on N_{si} at a constant bulk concentration of sticker groups (ϕ_{A-bulk} = 3.0 mol%, N = 80, interface thickness = 40), predicted from SCFLM. (filled diamonds: i = 1, filled squares: i = 2, filled triangles: i = 3, filled circles: i = bulk).

4. CONCLUSION

The peel energy of cPBD-AlS interfaces was examined through a T-peel test in terms of the sticker group concentrations (ϕ) and the interaction strength (χ_{P-S}) between sticker groups and the solid substrate. A critical concentration around 0.5 mol% was found giving maximum adhesion energy of 600 J/m^2, which is close to the peel energy of the PBD bulk. The bonding strength was strongly dependent on the annealing time as a consequence of the slow surface reorganization processes.

The dependence of the peel energy on ϕ and χ_{P-S} was elucidated through a SCFLM study, which was used to examine how sticker groups affect the interface structure. An interphase region was found adjacent to the solid substrate resulting from variation of chain connectivity and sticker group segregation. The modeling studies predicted how χ_{P-S} and ϕ affected the interphase structure and explained

the experimental data very well. Based on the modeling and experimental results, a schematic representation of interface structure was also proposed.

Acknowledgements

Financial support from National Science Foundation through contract DMR-9596-267 and Hercules Incorporated, Wilmington, Delaware, is gratefully acknowledged. We have benefited from many stimulating discussions and interactions with Dr. Selim Kusefoglu and Dr. Sri Bandyopadhyay.

References

[1] Wool, R. P., *Polymer Interfaces: Structure and Strength* (Hanser/Gardner, New York, 1995).
[2] Wool, R. P., In: *Performance of Plastics*, Brostow, W., Ed. (Hanser/Gardner, New York, in press), Chap. 15.
[3] *Short fibre-polymer composites* (Woodhead Publishing, Cambridge, England, 1996).
[4] Nagel-Baumgartner, J. and Cooper, S. L., *Biomaterials* **18**, 831–837 (1997).
[5] Palecek, S. P., Loftus, J. C., Ginsberg, M. H., Lauffenburger, D. A. and Horwitz, A. F., *Nature* **385**, 537–540 (1997).
[6] Lupinski, J. H. and Moore, R. S., In: *Polymeric Materials for Electronics Packaging and Interconnection, ACS Symposium Ser. No. 407* (American Chemical Society, Washington, DC, 1989), pp. 1–24.
[7] Gong, L., Friend, A. D. and Wool, R. P., *Macromolecules* **31**, 3706–3714 (1998).
[8] Creton, C., Kramer, E. J. and Hadiioannou, G., *Macromolecules* **24** 1846–1853 (1991).
[9] Brown, H. R., *Macromolecules* **26**, 1666–1670 (1993).
[10] Kramer, E. J., Norton, L. J., Dai, C. A., Sha, Y. and Hui, C. Y., *Faraday Discuss.* **98**, 31–46 (1994).
[11] Reichert, W. F. and Brown, H. R., *Polymer* **34**, 2289–2296 (1993).
[12] Creton, C., Kramer, E. J., Hui, C. Y. and Brown, H. R., *Macromolecules* **25**, 3075–3088 (1992).
[13] Xu, Z., Kramer, E. J., Edgecombe, B. D. and Frechet, J. M. J., *Macromolecules* **30**, 7958–7963 (1997).
[14] Deruelle, M., Tirrell, M., Marciano, Y., Hervet, H. and Leger, L., *Faraday Discuss.* **98**, 55–65 (1994).
[15] Deruelle, M., Leger, L. and Tirrell, M., *Macromolecules* **28**, 7419–7428 (1995).
[16] Lin, R., Wang, H., Kalika, D. S. and Penn, L. S., *J. Adhesion Sci. Technol.* **10**, 327–339 (1996).
[17] Lin, R., Quirk, R. P., Kuang, J. and Penn, L. S., *J. Adhesion Sci. Technol.* **10**, 341–349 (1996).
[18] Drzal, L. T., In: *Controlled Interphases in Composite Materials*, Ishida, H., Ed. (Elsevier, New York, 1990), pp. 309–320.
[19] Vanlandingham, M. R., McKnight, S. H., Palmese, G. R., Elings, J. R., Huang, X., Bogetti, T. A., Eduljee, R. F. and Gillespie, J. W. Jr., *Adhesion* **64**, 31–59 (1997).

[20] Chin, P., Mccullough, R. L. and Wu, W. L., *J. Adhesion* **64**, 145–160 (1997).
[21] Voros, G., Fekete, E. and Pukanszky, B., *J. Adhesion* **64**, 229–250 (1997).
[22] Bell, J. P., Schmidt, R. G., Malofsky, A. and Mancini, D., *J. Adhesion Sci. Technol.* **5**(10), 927–944 (1991).
[23] Brewis, D. M., *Int. J. Adhesion and Adhesive* **13**, 251–256 (1993).
[24] Cognard, J., *Int. J. Adhesion and Adhesives* **11**(2), 114–116 (1991).
[25] Sharpe, L. H., *Polymer Preprint* **37**(2), 52–53 (1996).
[26] Boerio, F. J., Davis, G. D., deVries, J. E., Miller, C. E., Mittal, K. L., Opila, R. L. and Yasuda, H. K., *Critical Reviews in Surface Chemistry* **3**(1), 81–99 (1993).
[27] Sharpe, L. H., *J. Adhesion* **67**(1–4), 277–289 (1998).
[28] Gong, L., Wool, R. P., Friend, A. D. and Goranov, K., *J. Polym. Sci., Part A: Polym Chem.* (1999), in press.
[29] Thomas, R. C., Houston, J. E., Crooks, R. M., Kim, T. and Michalske, T. A., *J. Am. Chem. Soc.* **117**, 3830–3834 (1995).
[30] Theodorou, D. N., *Macromolecules* **21**, 1411–1421 (1988).
[31] Theodorou, D. N., In: *Physics of Polymer Surfaces and Interfaces*; Sanchez, I. C., Ed. (Butterworth-Heinemann Manning, Greenwich, 1992), pp. 139–161.
[32] *BIOSYM/Molecular Simulations Manual*, Polymer 3.0.0, part 1, Chapter 6, pp. 1–38 (1995).
[33] Lewis, A. F. and Natarajan, R. T., In: *Polymer Science and Technology*, Lee, L.-H. Ed. (Plenum Press, New York, 1975), pp. 563–575.
[34] Mao, T. J. and Reegen, S. L., In: *Adhesion and Cohesion*: Weiss, P., Ed. (Elsevier, New York 1962), pp. 209–217.
[35] McLaren, A. D. and Seiler, C. J., *J. Polym. Sci.* **4**, 63–74 (1949).
[36] Schultz, J., Lavielle, L., Carre, A. and Comien, P., *J. Mater. Sci.* **24**, 4363–4369 (1989).
[37] Beck Tan, N. C., Peiffer, D. G. and Briber, R. M., *Macromolecules* **29**, 4969–4975 (1996).
[38] Gutman, L. and Chakraborty, A. K., *J. Chem. Phys.* **101**(11), 10074–10091 (1994).
[39] Gutman, L. and Chakraborty, A. K., *J. Chem. Phys.* **103**(24), 10733–10750 (1995).
[40] Roland, C. M. and Bohm, G. G., *Macromolecules* **18**, 1310–1314 (1985).
[41] Hamed, G. R. and Shieh, C. H., *Rubber Chem. Technol.* **57**, 227–242 (1984).
[42] O'Connor, K. and McLeish, T., *Faraday Discuss.* **98**, 67–78 (1994).